DOI: 10.4274/anatoljmed.2025.48343
Anatol J Gen Med Res 2025;35(3):321-329

CLINICAL RESEARCH / KLİNİK ARAŞTIRMA

ANATOLIAN JOURNAL of GENERAL MEDICAL RESEARCH

Keratocan and *Nicotinamide Mononucleotide Adenylyltransferase 1* are Prognostic Markers in Kidney Renal Papillary Cell Carcinoma

Keratokan ve *Nikotinamit Mononükleotit Adenililtransferaz 1* Renal Papiller Hücre Karsinomunda Prognostik Belirteçlerdir

Gülçin Çakan Akdoğan

Dokuz Eylül University, İzmir International Biomedicine and Genome Insitute, Department of Biomedicine and Health Technologies; İzmir Biomedicine and Genome Center, İzmir, Türkiye

Cite as: Çakan Akdoğan G. Keratocan and nicotinamide mononucleotide adenylyltransferase 1 are prognostic markers in kidney renal papillary cell carcinoma. Anatol J Gen Med Res. 2025;35(3):321-329

Abstract

Objectives: Keratan sulfate proteoglycans (KSPGs) are the least studied of the proteoglycans with emerging roles in cancer. Diverse roles of KSPGs are known; however, the KSPG interactome has not been defined to date. The aim here was to define a KSPG interactome and to determine biomarkers in cancer patients using published datasets and bioinformatic analysis tools.

Methods: The STRING database was utilized to compile a KSPG interactome centered around keratocan (KERA), lumican, fibromodulin and osteoglycin. STRING, Xena Browser, Gene Set Cancer Analysis Platform, and SmulTCan were used to perform data analyses.

Results: A 56-protein KSPG interactome network was discovered. Extracellular matrix (ECM) organization, PI3K-AKT signaling, ECM-receptor interactions, and nicotinamide metabolism pathways were enriched in the interactome. Multivariate prognostic modeling with Glmnet identified a seven-gene prognostic signature in kidney renal papillary cell carcinoma (KIRP), stratifying patients into distinct risk groups with strong predictive accuracy (area under the curve of 78.9%). Among these, *KERA* emerged as a biomarker of poor prognosis, while *nicotinamide mononucleotide adenylyltransferase 1 (NMNAT1)* emerged as a protective biomarker in KIRP.

Conclusion: This study describes a methodology to utilize available datasets for protein interactome discovery and for querying cancer prognostic genes. In this study, an extensive KSPG interactome was identified. This is the first report linking *KERA* and *NMNAT1* to prognosis in KIRP.

Keywords: KSPG, *keratocan*, *NMNAT1*, prognosis, kidney renal papillary cell carcinoma

Öz

Amaç: Keratan sülfat proteoglikanlar (KSPG'ler), kanserdeki rolleri en az çalışılmış proteoglikan grubudur. KSPG'lerin çeşitli işlevleri bilinmekle birlikte, KSPG etkileşim ağı (interaktom) bugüne kadar tanımlanmamıştır. Bu çalışmada, KSPG interaktomunun tanımlanması ve yayımlanmış veri setleri ile biyoinformatik analiz araçları kullanılarak kanser hastalarında prognostik açıdan önemli biyobelirteçlerin belirlenmesi amaçlanmıştır.

Yöntem: STRING veritabanı keratokan (KERA), lumikan, fibromodulin ve osteoglikan merkezli bir KSPG interaktomu oluşturmak için kullanılmıştır. Veri analizlerinde STRING, Xena Browser, Gene Set Cancer Analysis Platform ve SmulTCan araçları kullanılmıştır.

Address for Correspondence/Yazışma Adresi: Asst. Prof., Gülçin Çakan Akdoğan, Dokuz Eylül University, İzmir International Biomedicine and Genome Insitute, Department of Biomedicine and Health Technologies; İzmir Biomedicine and Genome Center, İzmir, Türkiye
E-mail: gulcin.cakan@ibg.edu.tr
ORCID ID: orcid.org/0000-0002-6356-5979

Received/Geliş tarihi: 02.10.2025
Accepted/Kabul tarihi: 04.11.2025
Published date/Yayınlanma tarihi: 30.12.2025

Öz

Bulgular: 56 proteinden oluşan bir KSPG etkileşim ağı keşfedilmiştir. Hücre dışı matriks (HDM) organizasyonu, PI3K-AKT sinyal yolu, HDM-reseptör etkileşimleri ve nikotinamid metabolizması interaktomda zenginleştirilmiş yollar arasında bulunmuştur. Glmnet ile yapılan çok değişkenli prognostik modelleme, böbrek renal papiller karsinom (KIRP) hastalarında yedi genlik bir prognostik imza ortaya koymuş; bu imza, hastaları güçlü prediktif doğrulukla (eğri altındaki alan %78,9) farklı risk gruplarına ayırmıştır. Bu analizde *KERA* kötü prognoz biyobelirteci olarak, *nikotinamit mononükleotit adenililtransferaz 1 (NMNAT1)* ise koruyucu bir biyobelirteç olarak öne çıkmıştır.

Sonuç: Bu çalışma, mevcut veri setlerinin protein interaktom keşfi ve kanser prognostik genlerinin belirlenmesinde nasıl kullanılabileceğini gösteren bir metodoloji sunmaktadır. Çalışma sonucunda kapsamlı bir KSPG interaktomu tanımlanmıştır. Bu, *KERA* ve *NMNAT1*'ın KIRP prognozu ile ilişkilendirildiğini gösteren ilk rapordur.

Anahtar Kelimeler: KSPG, *keratokan*, *NMNAT1*, prognoz, böbrek renal papiller hücrekarsinomu

Introduction

The extracellular matrix (ECM) surrounding the tumor is the first stromal component encountered by metastatic cancer cells before they move to distant sites. Traditionally considered a physical blockade, the ECM is now recognized as a dynamic regulator of tumor invasion, metastasis, and immune modulation. Increased ECM stiffness can suppress metastatic spread, whereas activation or overexpression of matrix metalloproteinases that digest the ECM has been associated with increased cellular migratory capacity and metastasis[1,2]. The influence of the ECM on metastatic cancer cells is complex, owing to its highly intricate and dynamic composition. The main macromolecular constituents are collagens and proteoglycans, both diverse groups that contribute to the organ- and tissue-specific composition of the ECM[3]. Proteoglycans are classified into several types, named after their glycosaminoglycan side chains, such as heparan sulfate, dermatan sulfate, or keratan sulfate. The determinants of the side chains are the specific types of disaccharide repeats, such as glucuronic acid or iduronic acid paired with glucosamine for heparan sulfates, and galactose paired with N-acetylglucosamine for keratan sulfates. Each proteoglycan molecule may have different lengths of disaccharide repeats, different sulfate loads on these repeats, and different core proteins[3]. Diversity in structure is likely to be reflected in functional diversity, making it especially challenging to pinpoint the roles of a particular proteoglycan[4].

Most research on the role of proteoglycans in cancer metastasis has focused on heparan sulfate proteoglycans[5]. Keratan sulfate proteoglycans (KSPGs), on the other hand, are the least studied in this context[6]. Recent transcriptomic studies have identified that *carbohydrate sulfotransferase 6 (CHST6)*, a keratan sulfate-specific sulfotransferase, is part of a genetic signature associated with poor prognosis in cancer[7-9]. Sulfation of KSPGs is a major influence on their function and solubility, as evidenced by the formation of KSPG aggregates in patients with macular corneal dystrophy, which is linked to *CHST6* mutations[10-12]. These data indicate that KSPG regulation is important in cancer progression.

Reports on the role of lumican (LUM) in cancer progression are contradictory[13]. *LUM* overexpression has been correlated with poor prognosis in colorectal, lung, and squamous cell carcinomas[14-17]. In contrast, *LUM* overexpression was shown to decrease the malignancy of melanoma cells and to correlate negatively with osteosarcoma tumor progression[18]. These contradictory findings may be related to the location of the KSPG: in the ECM or within the cancer cell itself. Additionally, differences in chain lengths and sulfation status of LUM in different cell types influence its interactions with other proteins and its roles[19].

KSPG binding proteins are not fully defined in the literature, as exemplified by the absence of a dedicated gene ontology (GO) term (https://www.ebi.ac.uk/QuickGO/). Proteoglycan binding GO term contains child terms that include syndecan binding (GO:0045545), chondroitin sulfate proteoglycan binding (GO:0035373), heparan sulfate proteoglycan binding (GO:0043395). This study aimed to define the KSPG interactome and to explore the expression and prognostic significance of its components in cancer, using published datasets and openly available bioinformatic tools and databases.

Here, KSPG-interacting proteins were identified through manual queries in STRING[20]. The STRING database integrates both experimentally validated interactions and computational predictions based on co-expression,

literature mining, and curated databases[20]. Then, data from The Cancer Genome Atlas (TCGA) Pan-Cancer study were analyzed using the SmulTCan app to investigate gene expression patterns and correlations with survival in cancer patients[21]. This analysis revealed a candidate prognostic gene set in the tumor microenvironment of kidney renal papillary cell carcinoma (KIRP).

Materials and Methods

KSPG Interactome Discovery

Selected KSPGs were manually entered into the STRING search query. Network display options were adjusted to reveal only high-confidence interactions, defined as the "physical subnetwork". A medium-confidence level was selected, and the first and second shells of the interactome were included in the network. Functional enrichment analysis was performed using STRING's built-in functions[20].

Statistical Analysis

The KSPG interactome gene set was queried in the Gene Set Cancer Analysis Platform (https://guolab.wchscu.cn/GSCA/#/), to evaluate the correlation of the KSPG interactome expression with drug sensitivity[22, 23].

Multivariate Prognostic Modeling

Gene expression and survival data of the TCGA Pan-Cancer study was retrieved from Xena Browser and uploaded to the SmulTCan app[21,24,25]. Univariate Cox proportional hazards (CPH) regression analyses and Glmnet analyses were performed for each cancer type[21]. Genes with p-values less than 0.05 were considered statistically significant. Forest plots were generated using Python (v3.10) with the matplotlib and seaborn libraries to visualize hazard ratios, 95% confidence intervals, and corresponding p-values.

Ethical Aspects of the Research

This research was conducted in accordance with the principles of the Declaration of Helsinki. Datasets available in public repositories were used. Therefore there is no ethical consern related to the work reported here.

Results

KSPG Interactome Discovery and Functional Enrichment Analysis

To compile a list of proteins interacting with KSPGs, the STRING database was queried for the four major KSPG core proteins: LUM, keratocan (KERA), fibromodulin (FMOD), and osteoglycin (OSG/mimecan). Experimentally validated interactors, as well as first- and second-shell interaction partners, were compiled (Table 1). LUM exhibited the largest interaction network, with experimentally validated interactors: zinc finger protein 488 (ZNF488), cystathionine gamma-lyase (CTH), and matrix metalloproteinase 14 (MMP14). The KERA subnetwork included direct physical interactors bleomycin hydrolase (BLMH), nudix hydrolase 12 (NUDT12), and EP300 interacting inhibitor of differentiation 2 (EID2). FMOD showed high-confidence binding to transforming growth factor-beta (TGFB) 1, and this binding extended to include other TGFB isoforms and matrix proteins. OSG was experimentally linked to collagen type XIV alpha 1

Table 1. Summary of KSPG interactome based on STRING analysis

KSPG name	Experimentally determined interactors	STRING network-1st shell	STRING network-2nd shell
Lumican	ZNF488, CTH, MMP14	BGN, COL1A1, COL1A2, COL3A1, COL5A1, COL5A2, COL5A3, COL11A1, COL11A2, COL16A1, FN1, TGFB1, TGFB2, ITGA2, ITGB1	ALB, DCN, FMOD, FASLG, BGN, POSTN
Keratocan	BLMH, NUDT12, EID2	BLMH, NUDT12, EID2, CXCL1, LUM	ACKR1, CXCL3, DPT, COL5A3, COL11A2, NMNAT1, NMNAT2, ENPP1, ENPP3, ZNF488
Fibromodulin	TGFB1	TGFB1, TGFB2, TGFB3, DCN, LUM, BGN, FN1, HSPG2, ACAN, ELN	–
Osteoglycin	COL14A1, SRC, HLA-DRB1, CNPY3	COL14A1, SRC, HLA-DRB1, CNPY3, OMD, VCAN, LPAR3	CDCP1, ADRB3, AFAP1, TNXB, NCAN, ACAN, TPBG, MLANA, CILP, CHRM1

Each row lists a core KSPG and its experimentally validated interactors, and the proteins found in its first and second-shell STRING network
Annotations are provided in Table S1

chain (COL14A1), proto-oncogene tyrosine-protein kinase Src (SRC), major histocompatibility complex, class II, DR beta 1 (HLA-DRB1), and canopy FGF signaling regulator 3 (CNPY3).

The identified KSPG interactome contains 56 proteins and forms a highly interconnected network that is visualized and functionally annotated using the STRING database (Figure 1A, Table S1). GO biological process enrichment analysis highlighted ECM organization as the most significantly enriched term [false discovery rate (FDR) <1e-23], with more than 20 genes contributing (Figure 1B). Closely related terms included extracellular structure organization, collagen fibril organization, and connective tissue development. Additional enrichment in cell adhesion and in positive regulation of smooth muscle cell proliferation was detected. Proteoglycans in cancer was the top KEGG pathway (FDR <1e-9), followed by focal adhesion, ECM-receptor interaction, phosphoinositide 3-kinase-AKT (PI3K-AKT) signaling, and TGFB signaling pathways, Interestingly, terms related to nicotinamide adenine dinucleotide (NADH) metabolism were enriched in both GO and KEGG pathway analyses.

Prognostic Associations of the KSPG Interactome Across Cancer Types

Correlation between mRNA expression profiles and drug sensitivity was assessed using the genomics of drug sensitivity in cancer portal and the Pan-Cancer dataset[23]. The top eight drugs with significant correlations with KSPG gene expression patterns and drug response were identified (Figure 2A, Table S2). Response to BHG712, a selective EphB4 inhibitor, was found to be strongly correlated with the expression levels of most genes in the KSPG interactome. Among these genes, *NMNAT2*, *ZNF488*, *TPBG*, *ITGB1*, *ITGB2*, *CDCP1*, and *FN1* were positively correlated, while *ENPP3*, *BLMH*, *HLA-DRB1*, and *CNPY3* were negatively correlated. Response to BRAF and MEK inhibitors (Dabrafenib, PLX4720, SB590885, CI-1040, and RDEA119) were negatively correlated with expression levels of *LUM*, *FN1*, *CXCL1*, *COL16A1*, *MMP14*, *HSPG2* and *MLANA*. Expression levels of the interactome genes in skin cutaneous melanoma (SKCM), uterine endometrial cancer (UCEC), and KIRP are plotted in Figure 2B. SKCM was chosen because the KSPG interactome gene set alteration frequency is highest (data not shown); UCEC and KIRP were chosen to complement CPH analyses explained below. Most KSPG genes are overexpressed in cancer patients. Among the core KSPGs, *LUM*, *FMOD*, and *biglycan* were highly overexpressed; *decorin*, *osteomodulin*, and *aggrecan* were moderately overexpressed; *KERA* was not overexpressed in the analyzed cancer types.

Next, CPH regression and Glmnet analyses were using the SmulTCan app across TCGA cancer types to define prognostic gene sets. The CPH analysis revealed specific multi-gene signatures in various cancer types, with uterine corpus endometrial carcinoma (UCEC) and KIRP exhibiting the most extensive lists of genes (Table S3). CPH predicted a highly significant multigene prognostic signature comprising 18 genes associated with survival in KIRP ($p<0.05$). These genes included the proteoglycans *LUM*, *FMOD*, and *KERA*, which are significantly associated with poor prognosis (Figure 3A). The metabolic genes *NMNAT1*, *NUDT12*, and *ENPP1* were significantly associated with a better prognosis. Other genes with prognostic value were *CXCL1*, *MLANA*, *CHRM1*, *ZNF488*, *BLMH*, and *CTH*. The model effectively stratified patients into high- and low-risk groups, which exhibited a significant difference in overall survival on the Kaplan-Meier plot (Figure 3B).

Next, the Glmnet method was applied to select the best gene subset; however, a fitted model was obtained only for KIRP. The KIRP prognostic signature included *KERA*, *ZNF488* and *CTH* with positive coefficients, suggesting their expression is associated with increased risk and poorer survival (Figure 3C). In contrast, *nicotinamide mononucleotide adenylyltransferase 1 (NMNAT1)* was assigned a negative coefficient, consistent with a protective effect. Additional low-magnitude positive coefficients were retained for *COL11A2*, *COL1A1*, and *COL5A2*. Receiver operating characteristic (ROC) curve analysis yielded an area under the curve (AUC) of 78.9%, indicating strong predictive accuracy (Figure 3D).

Discussion

KSPGs are found both extracellularly and intracellularly, with capacity to interact with a large number and variety of proteins[4]. Nevertheless, the experimental data on KSPG-interacting proteins are fragmented, and a definition of the KSPG interactome is needed. To address this gap, we used the STRING database to construct a physical interaction network centered on the KSPG core proteins KERA, LUM, FMOD, and OGN and identified a 56-protein KSPG interactome. The intereactome not only included ECM related proteins but also major cancer related pathways including PI3K-AKT signaling. Enrichment of focal adhesion, integrin binding, and TGFB binding may be linked to the structural remodeling required for cancer metastasis.

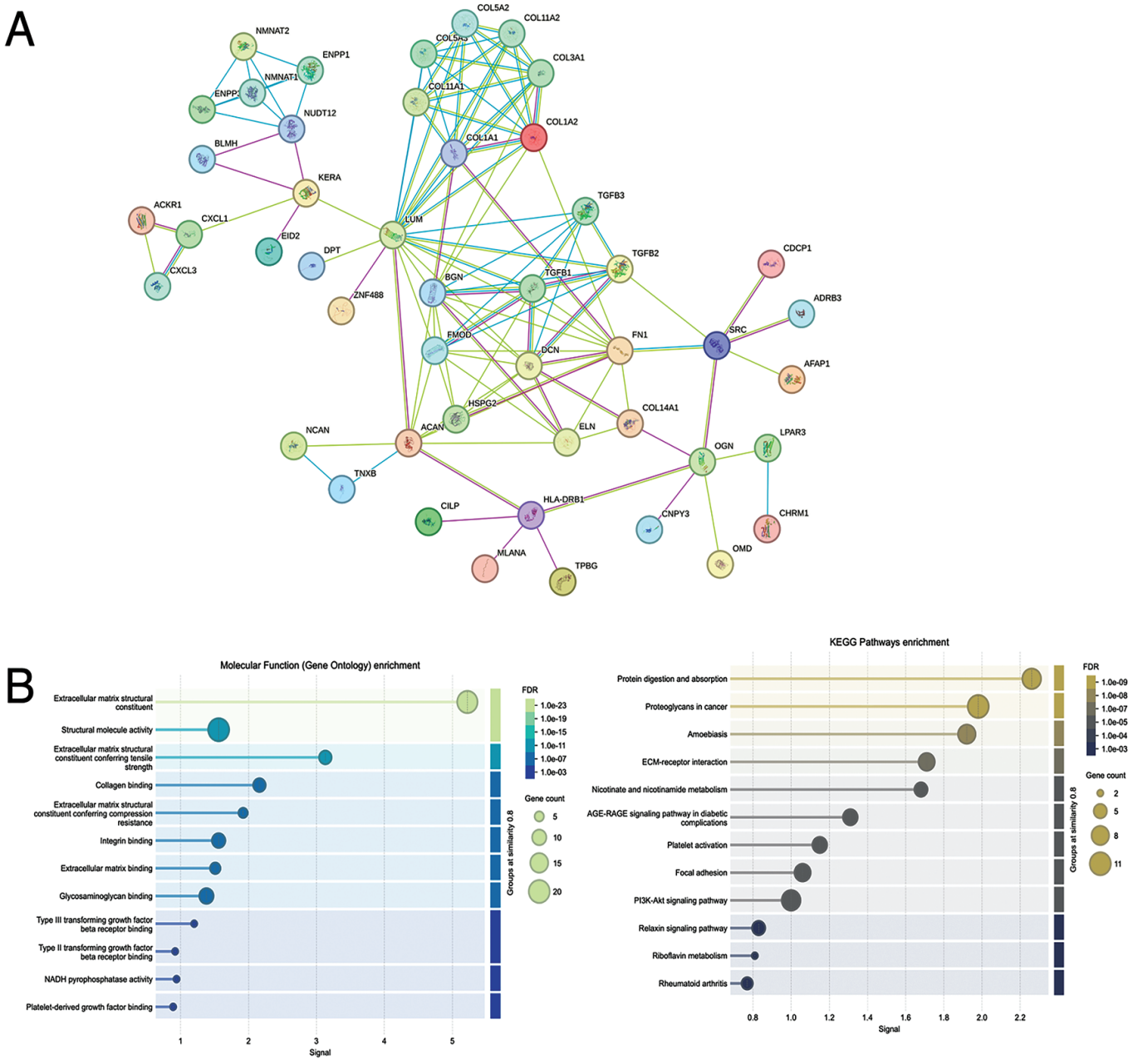

Figure 1. STRING-derived interaction network of the KSPG interactome

A) The network includes 56 proteins identified through STRING as part of the keratan sulfate proteoglycan (KSPG) interactome. Nodes represent proteins; edge colors indicate the type of supporting evidence: purple (experimentally determined interactions); blue (curated database associations); and green (text mining). **B)** GO biological process enrichment of the KSPG interactome. Bubble plot showing the top enriched GO biological processes. The x-axis represents gene ratio, while the y-axis lists the GO terms. Bubble size corresponds to the number of genes involved in each term; color intensity reflects statistical significance (FDR)

KSPG: Keratan sulfate proteoglycan, GO: Gene ontology, KEGG: Kyoto Encyclopedia of Genes and Genomes, FDR: False discovery rate

The composition of the ECM is known to modulate drug sensitivity in cancer[26]. Correlations between gene expression and BRAF-MEK inhibitors suggest a potential modulation of drug sensitivity via the KSPG interactome. The prognostic potential of KSPG interactome genes was analyzed via univariate CPH, and best subsets were selected using Glmnet multivariate penalized Cox regression. This approach enables simultaneous variable selection and regularization, identifying a minimal gene set with optimal predictive performance while excluding redundant or non-informative features[21]. The CPH approach identified numerous genes with significant associations with survival across tumor types, including uterine corpus endometrial carcinoma UCEC and KIRP. While this method is straightforward and sensitive to any gene-outcome association, it does not account for correlations among genes, potentially overestimating the

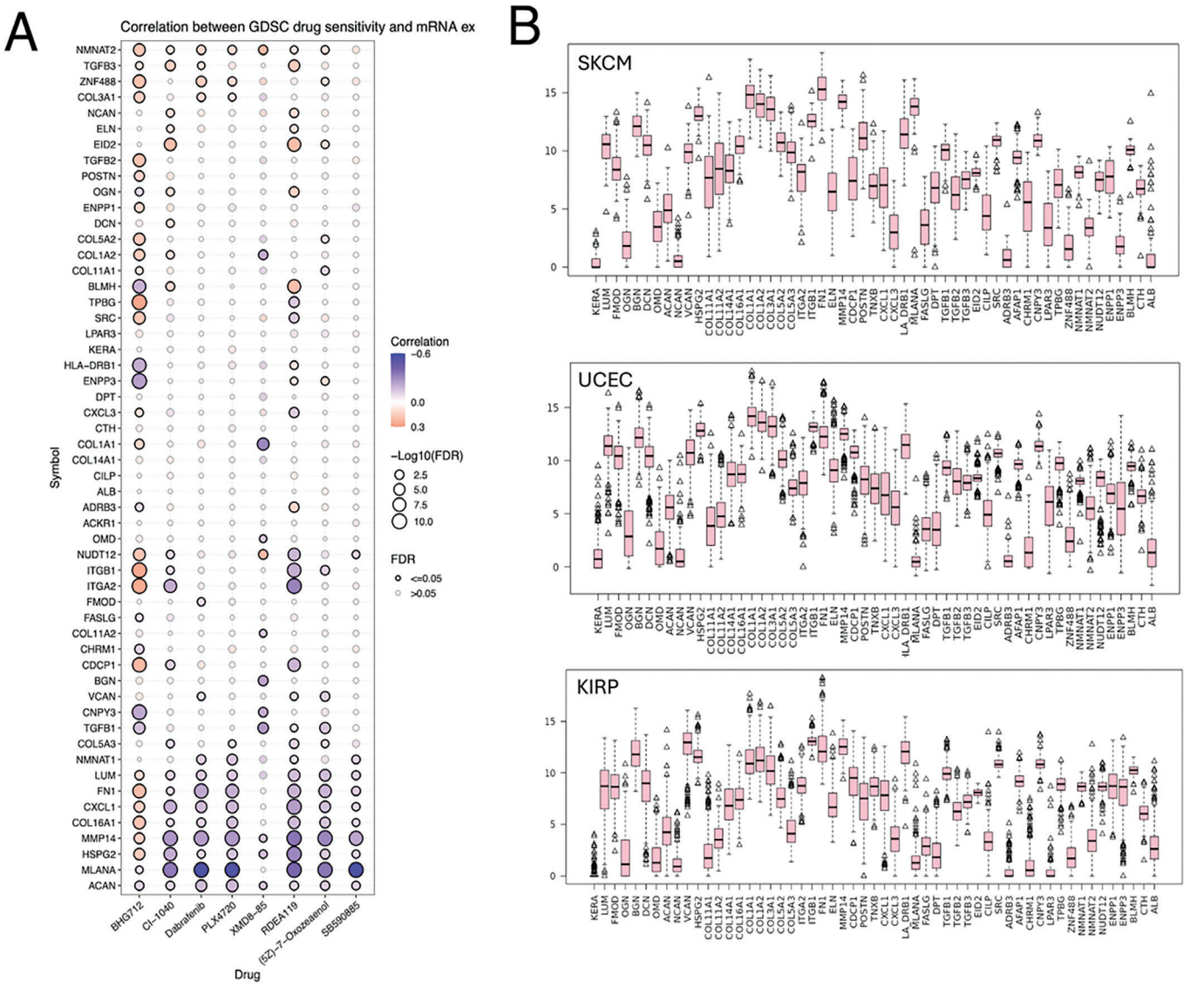

Figure 2. KSPG interactome expression in cancer

A) Drug sensitivity correlation figure summarizes the correlation between gene expression and the sensitivity of GDSC drugs (top 30) in Pan-Cancer (full list Table S2). B) Gene expression distribution of KSPG interactome genes in SKCM, UCEC and KIRP

GDSC: Genomics of drug sensitivity in cancer, KSPG: Keratan sulfate proteoglycan, SKCM: Skin cutenous melanoma, UCEC: Uterine endometrial cancer, KIRP: Kidney renal papillary cell carcinoma

number of relevant variables. By contrast, Glmnet applies lasso regularization to select a parsimonious multigene model with independent predictive contributions and improved generalizability[21]. However, this increased stringency can lead to failure to retain variables in the final model when predictors are highly correlated or when the incremental predictive value is modest relative to noise. This scenario occurred in UCEC, where no multigene signature was selected despite numerous univariate associations. However, in KIRP, Glmnet successfully identified a multigene signature consisting of *KERA*, *NMNAT1*, *ZNF488*, *COL5A2*, *COL1A1*, *COL11A2*, and *CTH*. The transcription factor *ZNF488* is functionally linked to *LUM* and *COL5A3* in the STRING network. Recently, the roles of *ZNF488* in cancer progression

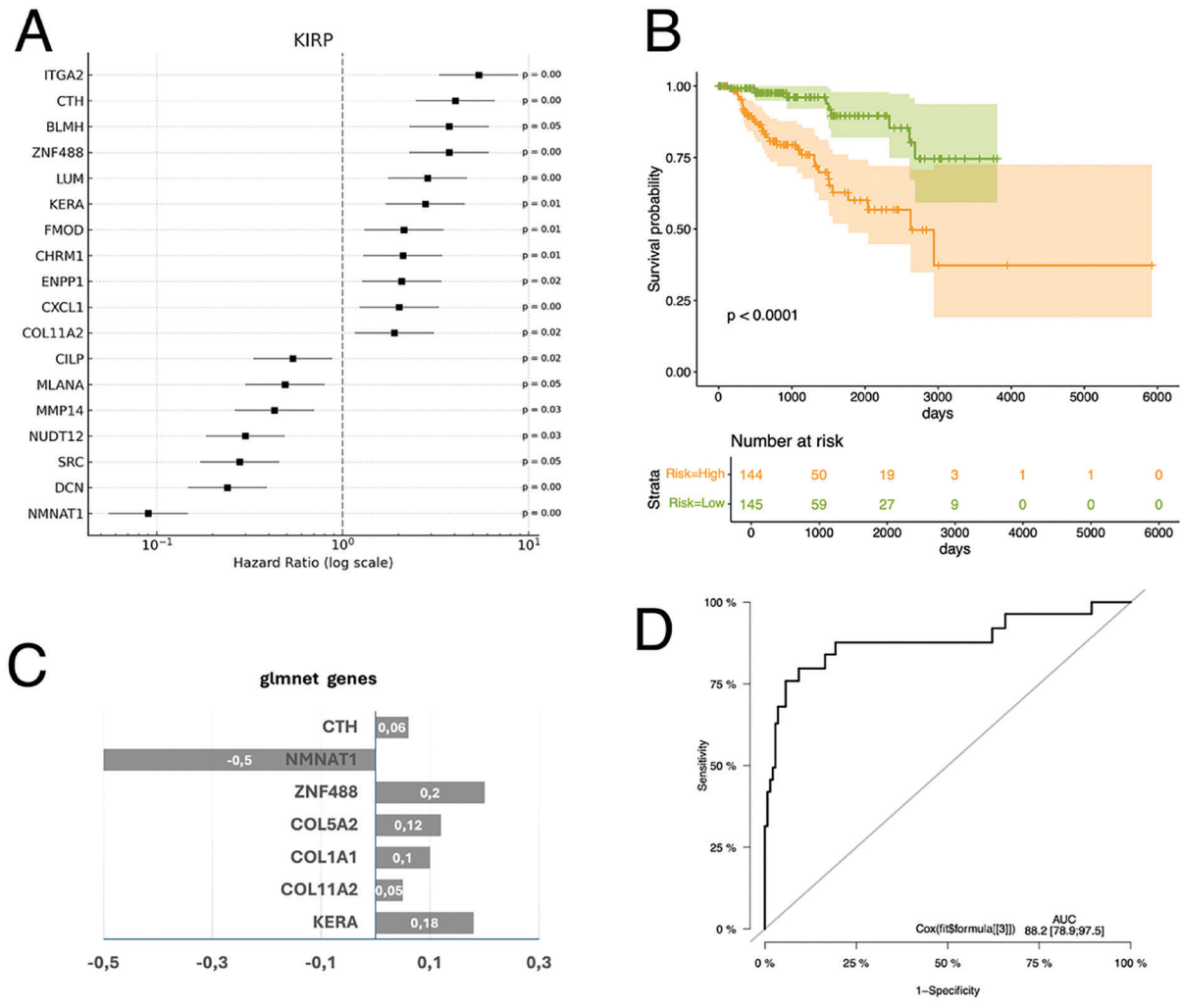

Figure 3. A prognostic gene signature is discovered in KIRP

A) Gene signature recovered with Cox modeling in KIRP. HRs and their 95% confidence intervals are displayed on a logarithmic scale. Genes with HR >1 are associated with poorer prognosis, while those with HR <1 are associated with improved survival. P-values are shown to the right of each gene. The gene order reflects increasing HR for visual clarity. **B)** Kaplan-Meier survival curves comparing overall survival between high-risk and low-risk groups. The high-risk group (orange) exhibited significantly poorer survival than the low-risk group (green) (log-rank p<0.0001). Shaded areas indicate 95% confidence intervals. Tick marks on the curves denote censored observations. The table below the plot shows the number of subjects at risk at each time point (in days). **C)** Prognostic gene signature discovered with Glmnet best subset selection. Coeficients are displayed on bar graph. **D)** ROC curve illustrating the predictive performance of the Glmnet model in distinguishing between the specified outcome groups. The AUC was 78.9%, indicating strong predictive accuracy. The diagonal dashed line represents the performance of a random classifier (AUC: 0.5)

KIRP: Kidney renal papillary cell carcinoma, HR: Hazard ratio, ROC: Receiver operating characteristic, AUC: Area under the curve

and resistance have been indicated, although the mechanism and its link to KSPGs have not been studied [27,28]. *KERA* had a positive coefficient, indicating that higher expression is associated with worse survival. Interestingly, *KERA* expression in KIRP is markedly lower than in other cancers and than that of other genes in the KSPG interactome. However, high variability in gene expression among patients was observed, suggesting that *KERA* expression must be kept very low for better patient prognosis.

KERA encodes a small leucine-rich proteoglycan involved in collagen organization and ECM architecture, but its role in cancer has been described in only a few studies[29,30]. *NMNAT1* had the most negative coefficient in the penalized model, suggesting a protective association in KIRP. Enrichment of the nicotinate and nicotinamide metabolism pathways suggested involvement of the KSPG network in regulating energy metabolism, which is further supported by the prognostic value of *NMNAT1* identified in this study. The NMNAT1 enzyme catalyzes a critical step in NAD^+ biosynthesis, potentially supporting metabolic homeostasis and resilience to oxidative stress. Notably, NMNAT1 is part of the KERA-centered STRING subnetwork together with NMNAT2, ENPP1, ENPP3, and NUDT12. These proteins regulate nicotinate and nicotinamide metabolism. Human NMNAT enzymes catalyze the formation of NAD^+ from adenosine triphosphate and nicotinamide mononucleotide (NMN) and the cleavage of NADH in the reverse reaction[31]. NUDT12 is a peroxisomal NADH pyrophosphatase and an mRNA-decapping enzyme that specifically removes the NAD cap from a subset of transcripts, thereby generating NMN and promoting mRNA decay, particularly under nutrient stress conditions[32,33]. It also hydrolyzes free NAD(P)H and diadenosine diphosphates to regulate peroxisomal nicotinamide nucleotide pools required for oxidative metabolism. Together, these findings suggest a potentially relevant ECM-metabolism regulatory axis, linking KERA and its interactors to energy metabolism and nucleotide turnover within the tumor microenvironment.

This analysis leveraged the SmulTCan web application, which integrates both univariate and multivariate survival modeling in an accessible interface[21]. SmulTCan proved particularly useful for rapidly evaluating prognostic associations without requiring advanced bioinformatics expertise or command-line tools, making it well suited for translational researchers and clinicians who wish to explore publicly available cancer datasets reproducibly. The methodology followed here illustrates that integrating curated protein interaction networks with public genomics data can reveal cancer-type-specific gene modules associated with prognosis and drug response.

Importantly, a KSPG interactome was identified and proposed in this study. *KERA* and *NMNAT1* were identified as having high prognostic value in KIRP, a finding not previously reported. Future studies are needed to functionally validate the contributions of the candidate genes identified here and to determine whether they can inform stratified therapeutic strategies or combination treatments that target ECM remodeling and tumor metabolism.

Ethics

Ethics Committee Approval: Datasets available in public repositories were used. Therefore there is no ethical consern related to the work reported here.

Informed Consent: This study does not involve any experiments conducted with patients, or patient materials, animals or animal materials. The researh was conducted with publicly available datasets.

Acknowledgements

Author thanks Prof. MD, Özlen Konu for critical reading of the manuscript and help with the SmulTCan App analyses.

Footnotes

Authorship Contributions

Concept: G.Ç.A., Design: G.Ç.A., Data Collection or Processing: G.Ç.A., Analysis or Interpretation: G.Ç.A., Literature Search: G.Ç.A., Writing: G.Ç.A.

Conflict of Interest: No conflict of interest was declared by the author.

Financial Disclosure: The author declared that this study received no financial support.

References

1. Wang M, Yang Y, Han L, et al. Effect of three-dimensional ECM stiffness on cancer cell migration through regulating cell volume homeostasis. Biochem Biophys Res Commun. 2020;528:459-65.
2. Deng B, Zhao Z, Kong W, Han C, Shen X, Zhou C. Biological role of matrix stiffness in tumor growth and treatment. J Transl Med. 2022;20:540.
3. Hardingham T. Proteoglycans and glycosaminoglycans. In: Seibel MJ, Bilezikian JP, Robins SP, (editors). Dynamics of bone and cartilage metabolism. 2nd ed. Elseiver; 2006:85-98.
4. Caterson B, Melrose J. Keratan sulfate, a complex glycosaminoglycan with unique functional capability. Glycobiology. 2018;28:182-206.

5. Wei J, Hu M, Huang K, Lin S, Du H. Roles of proteoglycans and glycosaminoglycans in cancer development and progression. Int J Mol Sci. 2020;21:5983.
6. Appunni S, Anand V, Khandelwal M, Gupta N, Rubens M, Sharma A. Small leucine rich proteoglycans (decorin, biglycan and lumican) in cancer. Clin Chim Acta. 2019;491:1-7.
7. Grant RC, Denroche RE, Borgida A, et al. Exome-wide association study of pancreatic cancer risk. Gastroenterology. 2018;154:719-22.
8. Xu F, Xu H, Li Z, et al. Glycolysis-based genes are potential biomarkers in thyroid cancer. Front Oncol. 2021;11:534838.
9. Liu G, Lu Y, Gao D, Huang Z, Ma L. Identification of an energy metabolism-related six-gene signature for distinguishing and forecasting the prognosis of low-grade gliomas. Ann Transl Med. 2023;11:146.
10. Melrose J. Keratan sulfate (KS)-proteoglycans and neuronal regulation in health and disease: the importance of KS-glycodynamics and interactive capability with neuroregulatory ligands. J Neurochem. 2019;149:170-94.
11. Basol M, Ersoz-Gulseven E, Ozaktas H, Kalyoncu S, Utine CA, Cakan-Akdogan G. Loss of carbohydrate sulfotransferase 6 function leads to macular corneal dystrophy phenotypes and skeletal defects in zebrafish. FEBS J. 2025;292:373-90.
12. Abbruzzese C, Kuhn U, Molina F, Rama P, De Luca M. Novel mutations in the *CHST6* gene causing macular corneal dystrophy. Clin Genet. 2004;65:120-5.
13. Appunni S, Rubens M, Ramamoorthy V, et al. Lumican, pro-tumorigenic or anti-tumorigenic: a conundrum. Clin Chim Acta. 2021;514:1-7.
14. Seya T, Tanaka N, Shinji S, et al. Lumican expression in advanced colorectal cancer with nodal metastasis correlates with poor prognosis. Oncol Rep. 2006;16:1225-30.
15. Matsuda Y, Yamamoto T, Kudo M, et al. Expression and roles of lumican in lung adenocarcinoma and squamous cell carcinoma. Int J Oncol. 2008;33:1177-85.
16. Xu W, Chen S, Jiang Q, et al. LUM as a novel prognostic marker and its correlation with immune infiltration in gastric cancer: a study based on immunohistochemical analysis and bioinformatics. BMC Gastroenterol. 2023;23:455.
17. Chen X, Li X, Hu X, et al. LUM expression and its prognostic significance in gastric cancer. Front Oncol. 2020;10:605.
18. Karamanou K, Franchi M, Proult I, Rivet R, Vynios D, Brezillon S. Lumican inhibits *in vivo* melanoma metastasis by altering matrix-effectors and invadopodia markers. Cells. 2021;10:841.
19. Chasan S, Hesse E, Atallah P, et al. Sulfation of glycosaminoglycan hydrogels instructs cell fate and chondral versus endochondral lineage decision of skeletal stem cells *in vivo*. Adv Funct Mater. 2021;32:2109176.
20. Szklarczyk D, Franceschini A, Wyder S, et al. STRING v10: protein-protein interaction networks, integrated over the tree of life. Nucleic Acids Res. 2015;43:D447-52.
21. Ozhan A, Tombaz M, Konu O. SmulTCan: a shiny application for multivariable survival analysis of TCGA data with gene sets. Comput Biol Med. 2021;137:104793.
22. Liu CJ, Hu FF, Xia MX, Han L, Zhang Q, Guo AY. GSCALite: a web server for gene set cancer analysis. Bioinformatics. 2018;34:3771-2.
23. Yang W, Soares J, Greninger P, et al. Genomics of drug sensitivity in cancer (GDSC): a resource for therapeutic biomarker discovery in cancer cells. Nucleic Acids Res. 2013;41:D955-61.
24. Goldman MJ, Craft B, Hastie M, et al. Visualizing and interpreting cancer genomics data via the Xena platform. Nat Biotechnol. 2020;38:675-8.
25. Hutter C, Zenklusen JC. The Cancer Genome Atlas: creating lasting value beyond its data. Cell. 2018;173:283-5.
26. Huang J, Zhang L, Wan D, et al. Extracellular matrix and its therapeutic potential for cancer treatment. Signal Transduct Target Ther. 2021;6:153.
27. Weng K, Li L, Zhou H. Transcription factor ZNF488 accelerates cervical cancer progression through regulating the MEK/ERK signaling pathway. Histol Histopathol. 2023;38:1381-90.
28. Chen D, Le SB, Manektalia H, et al. The EP3-ZNF488 axis promotes self-renewal of glioma stem-like cells to induce resistance to tumor treating fields. Cancer Res. 2025;85:360-77.
29. Chakravarti S. Focus on molecules: keratocan (KERA). Exp Eye Res. 2006;82:183-4.
30. Gao H, Qian R, Ren Q, et al. The upregulation of keratocan promotes the progression of human pancreatic cancer. Mol Cell Toxicol. 2024;20:271-80.
31. Sorci L, Scotti S, Peterlli R, et al. Initial-rate kinetics of human NMN-adenylyltransferases: substrate and metal ion specificity, inhibition by products and multisubstrate analogues, and isozyme contributions to NAD+ biosynthesis. Biochemistry. 2007;46:4912-22.
32. Grudzien-Nogalska E, Wu Y, Jiao X, et al. Structural and mechanistic basis of mammalian Nudt12 RNA deNADding. Nat Chem Biol. 2019;15:575-82.
33. Carreras-Puigvert J, Zitnik M, Jemth AS, et al. A comprehensive structural, biochemical and biological profiling of the human NUDIX hydrolase family. Nat Commun. 2017;8:1541.

Supplementary Table 1. https://d2v96fxpocvxx.cloudfront.net/cf9d60d6-523c-458a-a2e6-78728d3ffbb0/documents/Table%20S1_KSPGinteractome_annotation.xlsx

Supplementary Table 2. https://d2v96fxpocvxx.cloudfront.net/cf9d60d6-523c-458a-a2e6-78728d3ffbb0/documents/Table%20S3_CPH%20coefficients.xlsx

Supplementary Table 3. https://d2v96fxpocvxx.cloudfront.net/cf9d60d6-523c-458a-a2e6-78728d3ffbb0/documents/Table%20S2_GdscIC50_drug%20sensitivity_AndExprTable.xlsx